Baseline Map of Carbon Emissions from Deforestation in Tropical Regions

Nancy L. Harris *et al.*

Science **336**, 1573 (2012);
DOI: 10.1126/science.1217962

Science (print ISSN 0036-8075; online ISSN 1095-9203) is published weekly, except the last week in December, by the American Association for the Advancement of Science, 1200 New York Avenue NW, Washington, DC 20005.

(Fig. 3). A similar behavior is observed for the response in the momentum state population N_e (Fig. 4, inset), which exhibits a larger sensitivity to variations of the relative phase φ (*25*). For positive interaction V (Fig. 4, inset), the response of the system is reduced with respect to the non-interacting case, $V = 0$.

We have observed a roton-type mode softening causing a superfluid-to-supersolid transition in a model system for long-range interactions. Increasingly complex spatial structures of long-range atom-atom interactions (*28*–*30*) can be tailored by extending the experimental setup to multiple cavity modes.

References and Notes

1. I. Bloch, J. Dalibard, W. Zwerger, *Rev. Mod. Phys.* **80**, 885 (2008).
2. A. Griesmaier, J. Werner, S. Hensler, J. Stuhler, T. Pfau, *Phys. Rev. Lett.* **94**, 160401 (2005).
3. K.-K. Ni *et al.*, *Science* **322**, 231 (2008).
4. J. Deiglmayr *et al.*, *Phys. Rev. Lett.* **101**, 133004 (2008).
5. M. Lu, N. Q. Burdick, S. H. Youn, B. L. Lev, *Phys. Rev. Lett.* **107**, 190401 (2011).
6. T. Lahaye, C. Menotti, L. Santos, M. Lewenstein, T. Pfau, *Rep. Prog. Phys.* **72**, 126401 (2009).
7. L. Santos, G. V. Shlyapnikov, M. Lewenstein, *Phys. Rev. Lett.* **90**, 250403 (2003).
8. D. H. J. O'Dell, S. Giovanazzi, G. Kurizki, *Phys. Rev. Lett.* **90**, 110402 (2003).
9. R. W. Cherng, E. Demler, *Phys. Rev. Lett.* **103**, 185301 (2009).
10. N. Henkel, R. Nath, T. Pohl, *Phys. Rev. Lett.* **104**, 195302 (2010).
11. J. L. Yarnell, G. P. Arnold, P. J. Bendt, E. C. Kerr, *Phys. Rev. Lett.* **1**, 9 (1958).
12. Y. Pomeau, S. Rica, *Phys. Rev. Lett.* **72**, 2426 (1994).
13. T. Lahaye *et al.*, *Nature* **448**, 672 (2007).
14. M. Fattori *et al.*, *Phys. Rev. Lett.* **101**, 190405 (2008).
15. G. Bismut *et al.*, *Phys. Rev. Lett.* **105**, 040404 (2010).
16. T. Koch *et al.*, *Nat. Phys.* **4**, 218 (2008).
17. P. Münstermann, T. Fischer, P. Maunz, P. W. H. Pinkse, G. Rempe, *Phys. Rev. Lett.* **84**, 4068 (2000).
18. J. K. Asbóth, P. Domokos, H. Ritsch, *Phys. Rev. A* **70**, 013414 (2004).
19. C. Maschler, H. Ritsch, *Phys. Rev. Lett.* **95**, 260401 (2005).
20. S. Slama *et al.*, *AIP Conf. Proc.* **970**, 319 (2008).
21. P. Domokos, H. Ritsch, *Phys. Rev. Lett.* **89**, 253003 (2002).
22. D. Nagy, G. Szirmai, P. Domokos, *Eur. Phys. J. D* **48**, 127 (2008).
23. K. Baumann, C. Guerlin, F. Brennecke, T. Esslinger, *Nature* **464**, 1301 (2010).
24. J. Stenger *et al.*, *Phys. Rev. Lett.* **82**, 4569 (1999).
25. See supplementary materials on *Science* Online.
26. J. Steinhauer, R. Ozeri, N. Katz, N. Davidson, *Phys. Rev. Lett.* **88**, 120407 (2002).
27. P. Nozières, D. Pines, *The Theory of Quantum Liquids*, vol. II (Addison-Wesley, Reading, MA, 1990).
28. S. Gopalakrishnan, B. L. Lev, P. M. Goldbart, *Nat. Phys.* **5**, 845 (2009).
29. P. Strack, S. Sachdev, *Phys. Rev. Lett.* **107**, 277202 (2011).
30. S. Gopalakrishnan, B. L. Lev, P. M. Goldbart, *Phys. Rev. Lett.* **107**, 277201 (2011).

Acknowledgments: We thank H. Tureci, P. Domokos, and H. Ritsch for stimulating discussions. Supported by Synthetic Quantum Many-Body Systems (European Research Council advanced grant), Nanodesigning of Atomic and Molecular Quantum Matter (European Union, Future and Emerging Technologies open), National Centre of Competence in Research/Quantum Science and Technology, and the European Science Foundation (POLATOM).

Supplementary Materials

www.sciencemag.org/cgi/content/full/science.1220314/DC1
Supplementary Text
Fig. S1
References (*31*–*40*)

9 February 2012; accepted 2 May 2012
Published online 17 May 2012;
10.1126/science.1220314

Baseline Map of Carbon Emissions from Deforestation in Tropical Regions

Nancy L. Harris,[1]* Sandra Brown,[1] Stephen C. Hagen,[2] Sassan S. Saatchi,[3,4] Silvia Petrova,[1] William Salas,[2] Matthew C. Hansen,[5] Peter V. Potapov,[5] Alexander Lotsch[6]

Policies to reduce emissions from deforestation would benefit from clearly derived, spatially explicit, statistically bounded estimates of carbon emissions. Existing efforts derive carbon impacts of land-use change using broad assumptions, unreliable data, or both. We improve on this approach using satellite observations of gross forest cover loss and a map of forest carbon stocks to estimate gross carbon emissions across tropical regions between 2000 and 2005 as 0.81 petagram of carbon per year, with a 90% prediction interval of 0.57 to 1.22 petagrams of carbon per year. This estimate is 25 to 50% of recently published estimates. By systematically matching areas of forest loss with their carbon stocks before clearing, these results serve as a more accurate benchmark for monitoring global progress on reducing emissions from deforestation.

Although carbon emissions from fossil fuel use are relatively well quantified, emissions from land-use change—one of the largest anthropogenic sources of carbon to the atmosphere globally—are the most uncertain component of the global carbon cycle (*1*). The magnitude of these emissions has remained poorly constrained because of the use of different data, assumptions, and methodologies for estimating rates of deforestation, carbon stocks in vegetation and soils (*2*), the mode of clearing carbon, the fate of the cleared carbon, the response of the soil carbon pool to deforestation, and lag effects from historical land cover change (*3*).

Existing studies of the carbon balance of land-use change in tropical regions (*4*–*7*) incorporate carbon emissions from net changes in forest area, emissions from timber harvesting, and carbon removals from forest regrowth after abandonment. Statistics on net forest area changes and rates of timber harvesting, as reported by countries to the United Nations Food and Agriculture Organization (FAO), and a carbon cycle "bookkeeping" model were used to estimate net carbon emissions from the tropics as 1.9 and 2.2 petagrams of carbon per year (Pg C year^{-1}) for the 1980s and 1990s, respectively (*7*). Data reported to FAO are known to be unreliable (*8*), and the bookkeeping model uses many broad assumptions about the fate of cleared lands and their respective carbon stocks to estimate the associated net carbon impacts. The emergence and widespread use of multiresolution remote sensing imagery to track land-cover change resulted in new, lower estimates of net carbon emissions for the 1990s of 0.9 and 1.1 Pg C yr^{-1} (*9*, *10*), caused mainly from the use of different estimates of tropical deforestation rates. Recent studies (*11*, *12*) for the 2000s that use the bookkeeping model estimate average net emissions from tropical land-use change as 1.3 and 1.0 Pg C yr^{-1} (table S1).

Although these studies are useful for understanding the role of tropical land-use change in the global carbon cycle, a policy mechanism that proposes to compensate developing countries for reducing emissions from deforestation and forest degradation (REDD) will benefit from estimates of emissions from gross deforestation that are disaggregated from the forest regrowth term and that do not use a priori assumptions about the fate of vegetation carbon stocks after clearing (*4*–*7*, *9*–*12*). According to the FAO data and the bookkeeping model, gross emissions from tropical deforestation, without the inclusion of forest regrowth, are reported to be 2.8 ± 0.5 Pg C yr^{-1} for the period 2000 to 2007 and 2.2 Pg C yr^{-1} for the period 2000 to 2010 (table S1) (*11*, *12*). However, to inform ongoing policy discussions, more transparent and spatially explicit estimates of emissions are needed in which data for forest area loss and carbon stocks are assessed independently and the areas of forest loss are matched with the carbon stocks of the forests undergoing conversion.

Global loss in gross forest cover from 2000 to 2005 (*13*, *14*) and the spatial distribution of forest carbon stocks in tropical regions for the period circa 2000 (*15*) have been quantified by using

[1]Ecosystem Services Unit, Winrock International, Arlington, VA 22202, USA. [2]Applied GeoSolutions, Durham, NH 03824, USA. [3]Jet Propulsion Laboratory, California Institute of Technology, Pasadena, CA 91109, USA. [4]Institute of Environment, University of California, Los Angeles, Los Angeles, CA 90035, USA. [5]Department of Geographical Sciences, University of Maryland, College Park, MD 20742, USA. [6]The World Bank Group, Washington, DC 20433, USA.

*To whom correspondence should be sent. E-mail: nharris@winrock.org

multiscale remote sensing techniques, but they have not been used to estimate corresponding carbon emissions. We combined these data for 75 developing countries across three continental regions (Latin America, sub-Saharan Africa, and South and Southeast Asia) to develop a systematic, spatially consistent, and transparent estimate of gross carbon emissions from deforestation between 2000 and 2005 (*16*). We define deforestation as the area of forest cover removed because of any human or naturally induced disturbance (*16*). We use political rather than biome boundaries to define our study region (fig. S1) so as to provide consistent country-specific reference levels that can serve as a preliminary basis for emission reduction targets. Forest carbon stock estimates are partitioned into above- and belowground carbon density [megagrams of carbon per hectare (Mg C ha^{-1})] at 1-km spatial resolution, but the forest loss estimate is expressed in terms of the total area lost in 18.5-by-18.5-km blocks globally. We resolve the disparate spatial resolution of these two maps by repeating a randomization procedure in which forested 1-km pixels within a given 18.5-km block are selected randomly (n = 1000 realizations) until the forest loss quota (in hectares) for the block is met. The total carbon values of selected 1-km pixels (in megagrams of carbon) are then summed across the block to derive an emissions estimate. The average of the 1000 estimates associated with forest loss is assigned as the best estimate of emissions per 18.5-km block. By colocating biomass density data with forest loss data at relatively high spatial resolution, we improve on prior approaches that aggregate data at much coarser, regional scales (*12*). Additionally, a complete statistical uncertainty analysis around our final emissions estimate per block is generated by using a Monte Carlo–style sampling simulation that incorporates the uncertainty in above- and belowground carbon estimates at the 1-km scale and the uncertainty in the forest loss estimates at the 18.5-km scale (fig. S2). This method of quantifying uncertainty in carbon emissions is also an improvement on previous attempts that rely mainly on qualitative estimates based on expert opinion (*4*–*7*, *9*–*12*).

We estimated gross emissions resulting from gross loss in forest cover across the study region between 2000 and 2005 as 0.81 Pg C yr^{-1}, with a 90% prediction interval ranging from 0.57 to 1.22 Pg C yr^{-1}. This comprises 7 to 14% of total global anthropogenic CO_2 emissions over the time period analyzed. Forest loss in Latin America accounted for 54% of the total deforestation emissions, followed by 32% in South and Southeast Asia and 14% in sub-Saharan Africa. Our gross emissions estimate for tropical regions is approximately 25 to 50% of those reported previously for an overlapping time period by using the FAO/bookkeeping approach (Fig. 1) (*11*, *12*).

We reviewed the main sources of uncertainty in our analysis and conclude that the errors in estimating forest loss in tropical regions from coarse resolution satellite data and calibrated with higher resolution Landsat data (*13*, *14*) contributes ~5 to 10 times more to the total emissions uncertainty than the errors in estimates of forest

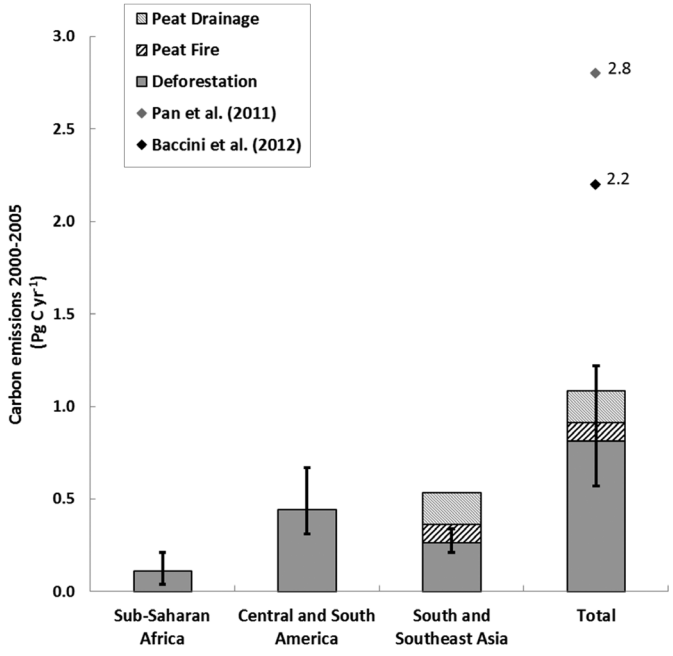

Fig. 1. Gross annual carbon emissions resulting from gross forest cover loss and peat drainage and burning between 2000 and 2005 compared with recently published estimates by (*11*) and (*12*) for an overlapping time period (2000–2007 and 2000–2010, respectively). Error bars represent 90% prediction intervals around median deforestation emission estimates. The estimates from (*11*) and (*12*) do not include peat emissions.

Table 1. Top carbon emitters from gross forest cover loss per region, 2000–2005. Countries are listed in order of highest to lowest carbon emissions between 2000 and 2005. Forest area and area loss values are based on (*14*), and average forest carbon density values are derived from (*15*).

Region	Country	Forest area 2000 (Mha)	Gross forest cover loss, 2000–2005 (Mha $year^{-1}$)	Average forest carbon density (Mg C ha^{-1})	Carbon emissions, 2000–2005 (Tg C $year^{-1}$)
Latin America and Caribbean	Brazil	458	3292	116	340
	Colombia	63	137	138	14
	Bolivia*	61	129	90	11
	Argentina*	49	437	24	10
	Venezuela*	49	115	134	9
Sub-Saharan Africa	Democratic Republic of the Congo	167	203	128	23
	Mozambique*	34	196	42	9
	Tanzania*	23	149	45	7
	Zambia	29	134	43	7
	Cameroon	26	54	142	7
South and Southeast Asia	Indonesia	107	701	155	105
	Malaysia	22	233	179	41
	Myanmar	33	186	155	29
	India	42	206	104	18
	Thailand	17	134	126	16

*Emission estimates (at 90% confidence) include potential emission values of zero in the uncertainty range.

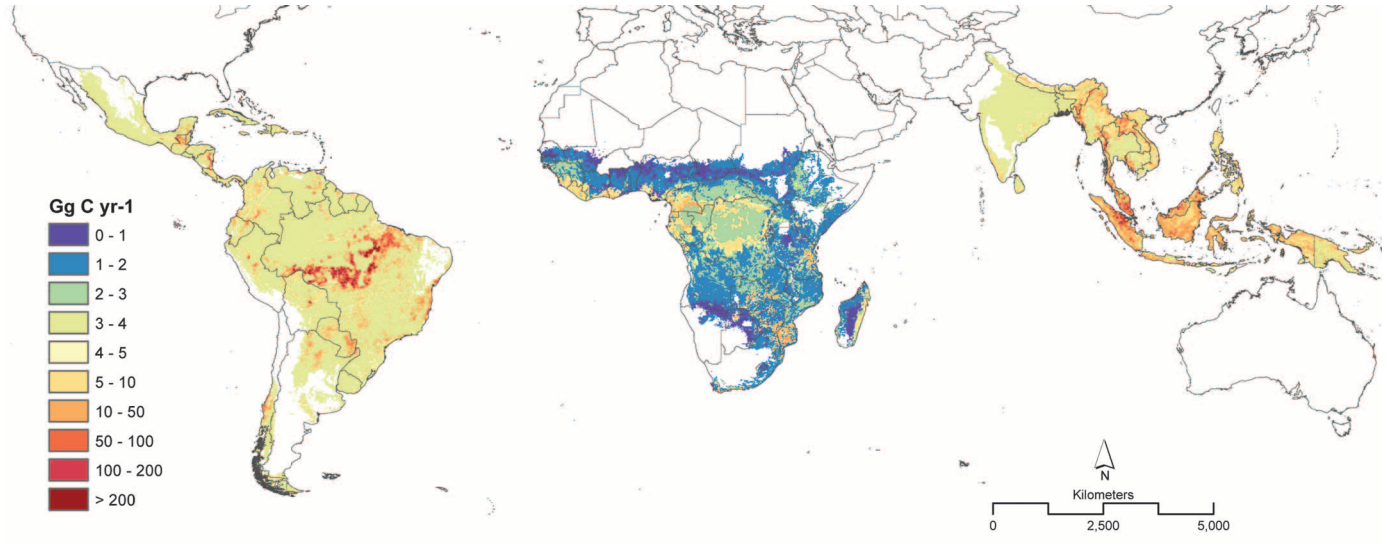

Fig. 2. Distribution of annual carbon emissions from gross forest cover loss between 2000 and 2005 mapped at a spatial resolution of 18.5 km.

carbon derived from aboveground biomass (*15*) and from the relationship between above- and belowground biomass (*17*), respectively. We focused our analysis on gross rather than net emissions because we can generate clear, statistically based uncertainty bounds around these estimates with the data and methods that are currently available. Net emission estimates require assumptions about the fate of converted lands to determine net carbon impacts that currently cannot be ascertained with statistical confidence across large regions. If robust data about the fate of converted lands existed and were used to generate a net emissions estimate, the result would be a reduction in our estimates of gross carbon emissions from deforestation shown in Fig. 1 (*16*).

Two countries—Brazil and Indonesia—produced the highest emissions between 2000 and 2005 and accounted for 55% of total emissions from tropical deforestation (Table 1). We present a map at the scale of analysis (18.5 by 18.5 km) (Fig. 2) to show the spatial distribution of emissions from tropical deforestation that captures the integrated importance of the extent of deforestation and the quantity of forest carbon stocks at regional scales. The relative importance of tropical Asia and Central and South America compared with tropical Africa as major sources of carbon to the atmosphere is shown in Fig. 2. Nearly 40% of total forest loss between 2000 and 2005 in our study region was concentrated in the dry tropics, but these losses accounted for only 17% of total carbon emissions, reflecting the low carbon density of these forests compared with tropical moist forests. Emissions are high in the Brazilian Amazon, but other areas of high emissions include Peninsular Malaysia, Laos, Sarawak (Malaysia), and Sumatra and Kalimantan (Indonesia) in Southeast Asia and, to a lesser extent, the Congo Basin in Africa.

The forest cover loss data used to derive the emissions estimates were generated by using a procedure based on a regression estimator (*13*, *14*) designed to produce aggregate estimates with reduced uncertainty for biomes, regions, and larger countries. Because forest loss estimates for individual 18.5-km blocks have relatively high uncertainty, we computed emissions at the aggregated country scale with less uncertainty (table S2) and present a relative ordering of emissions and relative uncertainty in emissions estimates by country (fig. S3). Our results for any 18.5-km block can be uncertain, but we are confident that the uncertainty estimation accurately bounds actual emissions at national and continental scales.

Our emission estimates reported above include those only from above- and belowground biomass carbon pools that generally account for 70 to 90% of total forest biomass carbon (*18*) and that we assume to occur immediately at the time of clearing. Other approaches (*4*–*7*, *9*–*12*) include the soil carbon pool and consider the carbon stocks in replacement vegetation because soil emissions can result when land is cleared and converted to cultivated crops, and emissions from deforestation could be partially offset by carbon accumulation in regrowing vegetation. Spatially explicit data exist for estimating soil carbon stocks and for identifying the replacement land use (*19*, *20*), but their precision is low, and the fate of the cleared land is difficult to ascertain accurately over large regions. Using standard methodologies (*21*), we conclude that accounting for soil carbon emissions increases our emissions estimate by less than 5%, and accounting for carbon accumulation in the replacement vegetation decreases our estimate by 5%, both of which fall within the uncertainty bounds of our analysis. Peat emissions are excluded from most estimates of emissions from land-use change (*4*–*7*, *9*–*12*), although peat drainage and burning in Southeast Asia have been shown to contribute a substantial portion of carbon emissions in past decades (*22*). Emissions from peat fire (*23*) and peat drainage (*24*) add another 0.099 and 0.173 Pg C yr^{-1}, respectively, which increases our total emissions estimate by approximately 25% but keeps the estimate within the uncertainty bounds of our analysis (Fig. 1).

Using the best available spatially consistent data sets on forest loss and forest carbon stocks, we have matched areas of forest loss with their carbon stocks before clearing to more accurately quantify gross emissions from deforestation in tropical regions. Our estimate is approximately 30% of previously published estimates for an overlapping time period. The largest source of uncertainty in our analysis is the estimates of gross forest-cover loss across large regions. This uncertainty in forest loss can be reduced through the detailed analysis of higher-resolution remotely sensed data. As developing countries collect and analyze new data to develop their reference levels for participation in a REDD mechanism, these data can be used to develop more accurate and precise estimates of country-scale emissions from all changes in forest cover. However, the current analysis will be useful as a benchmark against which progress on reducing emissions from deforestation may be assessed globally.

References and Notes

1. G. P. Peters *et al.*, *Nature Clim. Change* **2**, 2 (2012).
2. R. A. Houghton, K. T. Lawrence, J. L. Hackler, S. Brown, *Glob. Change Biol.* **7**, 731 (2001).
3. Y. Mahli, *Curr. Op. Environ. Sustain.* **2**, 237 (2010).
4. R. A. Houghton *et al.*, *Ecol. Monogr.* **53**, 235 (1983).
5. R. A. Houghton *et al.*, *Nature* **316**, 617 (1985).
6. R. A. Houghton, *Tellus* **51B**, 298 (1999).
7. R. A. Houghton, *Tellus* **55B**, 378 (2003).
8. A. Grainger, *Proc. Natl. Acad. Sci. U.S.A.* **105**, 818 (2008).

9. R. S. DeFries *et al.*, *Proc. Natl. Acad. Sci. U.S.A.* **99**, 14256 (2002).
10. F. Achard, H. D. Eva, P. Mayaux, H.-J. Stibig, A. Belward, *Global Biogeochem. Cycles* **18**, GB2008 (2004).
11. Y. Pan *et al.*, *Science* **333**, 988 (2011).
12. A. Baccini *et al.*, *Nature Clim. Change* **2**, 182 (2012).
13. M. C. Hansen *et al.*, *Proc. Natl. Acad. Sci. U.S.A.* **105**, 9439 (2008).
14. M. C. Hansen, S. V. Stehman, P. V. Potapov, *Proc. Natl. Acad. Sci. U.S.A.* **107**, 8650 (2010).
15. S. S. Saatchi *et al.*, *Proc. Natl. Acad. Sci. U.S.A.* **108**, 9899 (2011).
16. Materials and methods are available as supplementary materials on *Science* Online.
17. K. Mokany, R. J. Raison, A. S. Prokushkin, *Glob. Change Biol.* **12**, 84 (2006).
18. M. A. Cairns, S. Brown, E. H. Helmer, G. A. Baumgardner, *Oecologia* **111**, 1 (1997).
19. FAO/IIASA/ISRIC/ISSCAS/JRC. Harmonized World Soil Database (version 1.1); FAO, Rome, Italy and IIASA, Laxenburg, Austria (2009)
20. O. Arino *et al.*, GlobCover: ESA service for global land cover from MERIS. Geoscience and Remote Sensing Symposium (IEEE International, IGARSS 2007, 2007).
21. IPCC, IPCC guidelines for national greenhouse gas inventories (IGES, Japan, 2006; www.ipcc-nggip.iges.or.jp/public/2006gl/index.html).
22. S. E. Page *et al.*, *Nature* **420**, 61 (2002).
23. G. R. van der Werf *et al.*, *Proc. Natl. Acad. Sci. U.S.A.* **105**, 20350 (2008).
24. A. Hooijer *et al.*, *Biogeosciences* **7**, 1505 (2010).

Acknowledgments: Funding for this work was provided to Winrock International under contract 7150484 by the World Bank's World Development Report 2010: Development and Climate Change. The findings, interpretations, and conclusions expressed in this paper are entirely those of the authors. They do not necessarily represent the views of the World Bank and its affiliated organizations or those of the Executive Directors of the World Bank or the governments they represent. Support for the forest cover loss mapping work was provided by National Aeronautics and Space Administration's Land Cover and Land Use Change and MEASURES programs under grants NNG06GD95G and NNX08AP33A. The authors would like to thank K. Mokany for providing the original data used to derive relationships between above- and belowground biomass. Forest loss data are available at http://globalmonitoring.sdstate.edu/projects/gfm. Carbon stock data are available at http://carbon.jpl.nasa.gov. Emissions data are available at www.appliedgeosolutions.com/science-paper.html.

Supplementary Materials

www.sciencemag.org/cgi/content/full/336/6088/1573/DC1
Materials and Methods
Figs. S1 to S3
Tables S1 and S2
References (*25*–*29*)

15 December 2011; accepted 3 May 2012
10.1126/science.1217962

Endophytic Insect-Parasitic Fungi Translocate Nitrogen Directly from Insects to Plants

S. W. Behie,[1] P. M. Zelisko,[2] M. J. Bidochka[1]*

Most plants obtain nitrogen through nitrogen-fixing bacteria and microbial decomposition of plant and animal material. Many vascular plants are able to form close symbiotic associations with endophytic fungi. *Metarhizium* is a common plant endophyte found in a large number of ecosystems. This abundant soil fungus is also a pathogen to a large number of insects, which are a source of nitrogen. It is possible that the endophytic capability and insect pathogenicity of *Metarhizium* are coupled to provide an active method of nitrogen transfer to plant hosts via fungal mycelia. We used soil microcosms to test the ability of *M. robertsii* to translocate insect-derived nitrogen to plants. Insects were injected with ^{15}N-labeled nitrogen, and we tracked the incorporation of ^{15}N into amino acids in two plant species, haricot bean (*Phaseolus vulgaris*) and switchgrass (*Panicum virgatum*), in the presence of *M. robertsii*. These findings are evidence that active nitrogen acquisition by plants in this tripartite interaction may play a larger role in soil nitrogen cycling than previously thought.

Nitrogen gas, although it constitutes 78% of the atmosphere, is unavailable to plants as a source of nitrogen unless it is fixed by microbial symbionts (e.g., *Rhizobium*) or free-living microbes (e.g., *Azotobacter*) (*1*). In many natural as well as agricultural settings, nitrogen is the limiting nutrient for plant growth. The current model of the soil nitrogen cycle relies heavily on nitrogen-fixing bacteria to furnish plants with usable nitrogen (some is fixed by lightning strikes) (*2*). However, there are some examples in which plants have evolved mechanisms to scavenge nitrogen from insects. Carnivorous plants are able to obtain substantial amounts of nitrogen from insects they ingest. Pitcher plants (families Nepenthaceae and Sarraceniaceae) trap insects in a deep cavity filled with liquid, and insect-derived nitrogen can constitute up to 70% of the plant nitrogen content (*3*). In one known case of fungus-mediated transfer of insect-derived nitrogen to plants, the ectomycorrhizal fungus *Laccaria bicolor* transfers nitrogen from soil-dwelling collembola to white pine (*Pinus strobus*) whose roots it colonizes (*4*).

The ability of *L. bicolor* to transfer insect-derived nitrogen was specific to white pine, and generally *L. bicolor* associates with roots of pine and spruce in temperate forests (*5*, *6*). Nonetheless, these findings suggest that a more general example of insect-derived nitrogen transfer via fungal mycelia to plants may exist. *Metarhizium* spp. are ubiquitous soil-dwelling insect-pathogenic fungi that are found in a variety of ecosystems worldwide (*7*), occur in soils up to 10^6 propagules per gram (*8*), and can infect more than 200 species of insects (*9*). Insects contribute substantial amounts of nitrogen to soil. Each square meter of habitat can provide 0.4 to 4 g (by weight) of available insect nitrogen (see supplementary text).

During a routine survey of plant root symbionts, we found that *Metarhizium* spp. formed endophytic associations with many plant species (*10*, *11*). Endophytes live internally within the plant, and the host plant may benefit from the interaction (*12*). Here, we hypothesized that *Metarhizium* can parasitize and kill a soil-born insect, then transfer the insect-derived nitrogen to plants via fungal mycelia and endophytic association.

We used ^{15}N-labeled waxmoth (*Galleria mellonella*) larvae as a model prey insect and used this model in the experimental design to measure *Metarhizium*-mediated translocation of ^{15}N to the foliage of haricot bean (*Phaseolus vulgaris*) or switchgrass (*Panicum virgatum*). ^{15}N-labeled waxmoth larvae were added to microcosms in which the roots of the plants were separated from each insect by means of a 30-μm mesh (fig. S1). The insects were infected by *Metarhizium* 48 hours after ^{15}N injection and then placed into the microcosm, and the amount of ^{15}N transfer to plant tissues was determined during a 1-month period. After 14 days, in the presence of *Metarhizium*, insect-derived nitrogen constituted 28% and 32% of the nitrogen content in haricot bean and switchgrass, respectively; this represented significantly greater ^{15}N incorporation than in the presence of uninfected ^{15}N-labeled waxmoth larvae [Fig. 1, factorial analysis of variance (ANOVA), $P < 0.01$]. After 28 days, insect-derived nitrogen constituted 12% and 48% of bean and switchgrass nitrogen content, respectively, in the presence of *Metarhizium*; this again represented significantly greater ^{15}N incorporation than in the presence of uninfected ^{15}N-labeled waxmoth larvae (Fig. 1; factorial ANOVA, $P < 0.05$). Similar results were observed when the plant seeds were first inoculated with conidia of *Metarhizium* and subsequently formed a root endophytic association. We therefore concluded that

[1]Department of Biological Sciences, Brock University, St. Catharines, Ontario L2S 3A1, Canada. [2]Department of Chemistry, Brock University, St. Catharines, Ontario L2S 3A1, Canada.

*To whom correspondence should be addressed. E-mail: mbidochka@brocku.ca